Manipulating 4*f* quadrupolar pair-interactions in TbB_2C_2 using a magnetic field

A. M. Mulders,[1,2,3] U. Staub,[1] V. Scagnoli,[1] Y. Tanaka,[4] A. Kikkawa,[4] K. Katsumata,[4] and J. M. Tonnerre[5]
[1]*Swiss Light Source, Paul Scherrer Institut, 5232 Villigen PSI, Switzerland*
[2]*Department of Imaging and Applied Physics, Curtin University of Technology, Perth, Western Australia 6845, Australia*
[3]*The Bragg Institute, Australian Nuclear Science and Technology Organization, Lucas Heights, New South Wales 2234, Australia*
[4]*RIKEN SPring-8 Center, Harima Institute, Sayo, Hyogo 679-5148, Japan*
[5]*CNRS Grenoble, 38042 Grenoble Cedex 9, France*
(Received 22 December 2006; revised manuscript received 30 April 2007; published 30 May 2007)

Resonant soft-x-ray Bragg diffraction at the Tb $M_{4,5}$ edges and nonresonant Bragg diffraction have been used to investigate orbitals in TbB_2C_2. The Tb 4*f* quadrupole moments are ordered in zero field below T_N and show a ferroquadrupolar alignment dictated by the antiferromagnetic order. With increasing applied field along [110], the Tb 4*f* magnetic dipole moments rotate in a gradual manner toward the field. The quadrupole moment is rigidly coupled to the magnetic moment and follows this field-induced rotation. The quadrupolar pair-interaction is found to depend on the specific orientation of the orbitals as predicted theoretically and can be manipulated with an applied magnetic field.

DOI: 10.1103/PhysRevB.75.184438 PACS number(s): 75.40.Cx, 71.70.Ch, 78.70.Ck

I. INTRODUCTION

Correlation between conduction electrons and electronic orbitals leads to interesting materials properties such as metal-insulator transitions, colossal magnetoresistance, and superconductivity. Aspheric electronic orbitals, characterized by their quadrupole moment, may order and cause partial charge localization of the conduction electrons[1] or mediate coupling between Cooper pairs.[2] Orbital order in *f*-electron materials is dominated by coupling with the lattice (Jahn-Teller) or by indirect Coulomb interactions via the conduction electrons. That the latter can be important for intermetallic compounds was established theoretically,[3,4] but detailed experimental knowledge is limited due to the difficulty observing the associated orbital excitations. A recent neutron-diffraction study provided evidence of a modulated quadrupolar motif in $PrPb_3$, believed to be a direct consequence of indirect Coulomb interactions exhibiting oscillatory nature.[5] The large orbital momentum of the *f* electronic shell also gives rise to a significant influence of higher multipole moments and may lead to hidden order phase transitions as demonstrated in the extensively studied URu_2Si_2.[6] Therefore, it is important to understand the quadrupolar and higher-order multipole pair-interactions in these materials.

Quadrupolar order has been successfully investigated using neutron scattering in applied fields where induced magnetic moments reveal the underlying quadrupolar arrangement or motif. In addition, the relatively weak nonresonant x-ray-diffraction intensity of the quadrupole moments can be observed using synchrotron techniques allowing a *direct* determination of orbital motifs.[7,8]

Resonant x-ray scattering at the $L_{2,3}$ edge provided the first proof of the orbital motif in DyB_2C_2.[9,10] TbB_2C_2 is proposed to exhibit a transition from antiferromagnetic (AFM) to antiferroquadrupolar (AFQ) order in an applied magnetic field[11] and is therefore an interesting candidate for investigation of its orbital interactions.

A magnetic field is time odd and cannot couple to quadrupole moment, which is time even, but nevertheless in TbB_2C_2 the ordering temperature increases to 35 K, well above T_N=21.7 K, in an applied magnetic field of 10 T. Consequently, the interplay between dipole (time-odd) and quadrupole (time-even) moments can be readily investigated. Neutron-diffraction studies revealed similarities between the magnetic structure in applied fields and the magnetic structure in the combined AFQ and AFM phase of DyB_2C_2.[12]

To test the suggested field-induced quadrupolar ordering, we have investigated TbB_2C_2 in an applied magnetic field *H* with x-ray scattering techniques. We show that orbital order is present in the AFM phase of TbB_2C_2 at zero field, however, with ferroquadrupolar alignment, which is dictated by the AFM structure. The quadrupoles are rigidly linked to the magnetic dipole moments and rotate with *H* along the [110] direction. We show that, due to this rotation, the quadrupole pair-interactions become stronger with applied field.

II. EXPERIMENT

A single crystal of TbB_2C_2 was grown by Czochralski method using an arc furnace with four electrodes. Samples were cut and polished perpendicular to the [001] direction. The $(00\frac{1}{2})$ reflection was recorded at the Tb $M_{4,5}$ edges of TbB_2C_2 at the RESOXS end station of the SIM beamline at the Swiss Light Source of the Paul Scherrer Institut. A permanent magnet provided a field of 1 T parallel to the [110] direction in the scattering plane. In addition, nonresonant x-ray Bragg diffraction of the $(01\frac{l}{2})$ and $(11\frac{l}{2})$ reflections was performed at the BL19LXU beamline at SPring-8 with 30 keV x rays using a Ge solid-state detector to eliminate higher-order harmonics. A cryomagnet provided *H* along the [110] direction. Structure factors were derived from the integrated intensity, corrected for polarization, Lorenz factor, absorption, and sample geometry.

III. RESULTS

The energy dependence of the $(00\frac{l}{2})$ reflection recorded at the Tb $M_{4,5}$ edges in zero field is shown in Fig. 1(a). The

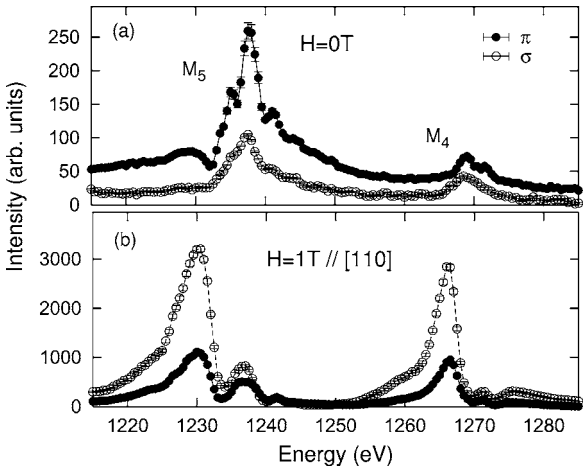

FIG. 1. Energy profile of the $(00\frac{l}{2})$ reflection at the Tb $M_{4,5}$ edges in TbB_2C_2 in (a) zero field and (b) applied field of 1 T along [110], recorded with σ or π incident radiation at 11 K.

incident polarization is chosen either perpendicular to (σ) or in the scattering plane (π), while the sum of both transmitted polarizations (σ', π') is recorded. While polarization analysis has been developed recently for the $3d$ $L_{2,3}$ edges,[13,14] analyzer efficiency at the Tb $M_{4,5}$ edges is too low for the current experiment. A significant part of the scattered intensity is due to the total reflectivity of the polished sample. The $(00\frac{l}{2})$ intensity disappears around 23 K consistent with the magnetic ordering temperature, and its energy profile is independent of sample rotation about the Bragg wave vector. In contrast, the diffracted intensity with $H=1$ T, along the [110] direction, shown in Fig. 1(b), is much stronger and strongest for incoming σ radiation. The energy profile is independent of temperature and the $(00\frac{1}{2})$ reflection vanishes above 22 K.

Nonresonant Bragg intensities have been recorded for various $(01\frac{l}{2})$ and $(11\frac{l}{2})$ reflections as function of temperature and applied field. In zero applied magnetic field, the $(01\frac{l}{2})$-type reflections are observed below 21 K while the $(11\frac{l}{2})$-type reflections are absent. The temperature dependence of the $(01\frac{9}{2})$ and $(11\frac{15}{2})$ reflections has been recorded at applied field of 5 T, while the magnetic-field dependence was recorded at 15 and 27 K. The intensity of the $(11\frac{15}{2})$ is zero at zero field and that of $(01\frac{9}{2})$ is very weak compared to its intensity in applied magnetic fields.

Figures 2(a) and 2(b) show the structure factors that relate directly to the order parameter, obtained from the integrated, nonresonant Bragg intensities of the $(01\frac{9}{2})$ and $(11\frac{15}{2})$ reflection as a function of applied field. In the AFM phase, at 15 K, the structure factors show a linear increase for applied fields below 1.5 T. In the paramagnetic phase, at 27 K, the ordered phase is entered above 3 T. The $(01\frac{9}{2})$ reflection appears at 3.2 T, while the $(11\frac{15}{2})$ reflection appears at 3.5 T. However, the evolution of the structure factor with increasing field is smooth for both reflections without a hint of a phase transition at 3.5 T for $(01\frac{9}{2})$. A similar behavior is observed as function of temperature in an applied field of 5 T (not shown). The intensities of $(01\frac{9}{2})$ and $(11\frac{15}{2})$ show a

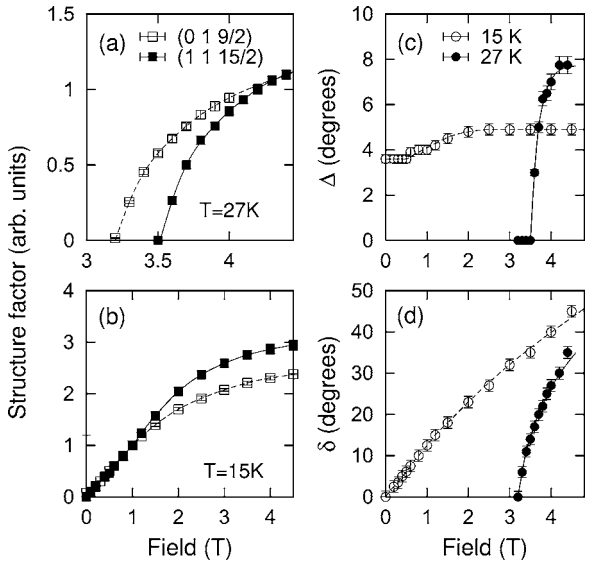

FIG. 2. Structure factor of the $(01\frac{9}{2})$ and $(11\frac{15}{2})$ reflection as function of applied magnetic field recorded with 30 keV at (a) $T=27$ K and (b) $T=15$ K. (c) and (d) show the deduced angles of Tb $4f$ orbital rotation as defined in Fig. 3.

smooth decrease with increasing temperature and disappear above 30 and 29.5 K, respectively.

IV. DISCUSSION

First we discuss the nonresonant Thomson Bragg diffraction results [Figs. 2(a) and 2(b)] and demonstrate that the quadrupole moment follows the magnetic-moment rotation in applied fields. It is remarkable that the temperature and magnetic-field dependences of the structure factor of both the $(01\frac{9}{2})$ and $(11\frac{15}{2})$ reflections are smooth while their transition temperatures are different. A structural transition with alternating displacements of the B and C atoms gives intensity in both types of reflections[7] and cannot account for the present observation of intensity at $(01\frac{9}{2})$ and the absence of intensity at $(11\frac{15}{2})$. Magnetic, or time-odd, x-ray diffraction is generally weak and does not explain the magnitude of the observed intensity. We conclude that the scattering arises from time-even x-ray diffraction, i.e., from the aspheric charge distribution of the $4f$ shell, as such scattering can be significantly more intense.[8]

To determine the Thomson structure factor, it is assumed that the Tb ion on each site has the same charge distribution except for its specific orientation. Using the formalism for nonresonant time-even scattering of Lovesey *et al.*,[15] we deduce that two independent Tb ions contribute and obtain the following for the structure factors:

$$F_{11\frac{l}{2}} \propto -2[\sin(2\phi_1) - \sin(2\phi_3)]\langle Q_{11\frac{l}{2}}\rangle, \tag{1}$$

$$F_{01\frac{l}{2}} \propto [\cos(2\phi_1) - \cos(2\phi_3)]\langle Q_{01\frac{l}{2}}\rangle, \tag{2}$$

when the Miller index l equals an odd integer. The principal axis of the $4f$ orbital at atom n is canted in the ab plane with respect to the [100] direction with angle ϕ_n. $\langle Q_{hkl}\rangle$ is the

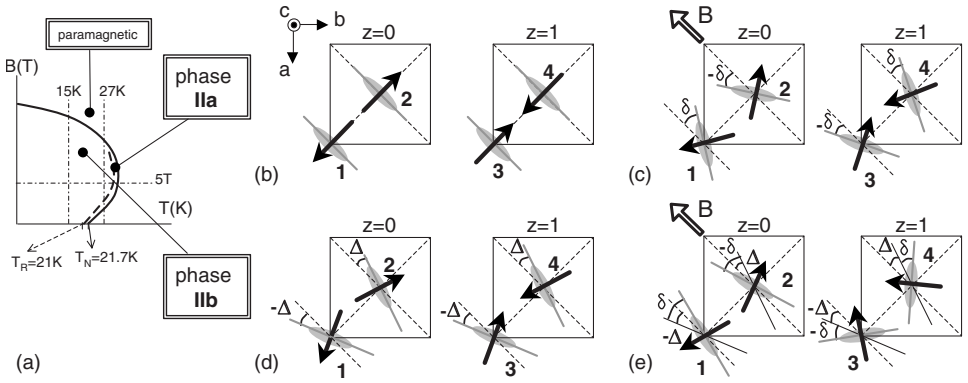

FIG. 3. (a) Phase diagram of TbB_2C_2 with magnetic field applied along [110]. (b) and (c) illustrate the orientation of magnetic moments (arrows) and quadrupole moments (ovals) in TbB_2C_2 in phase IIa in zero field and under applied fields, respectively. (d) and (e) illustrate phase IIb under the same conditions.

expectation value of the Tb 4*f* time-even multipolar moment for a given field, temperature, and Bragg wave vector $\mathbf{k}=(k_a,k_b,k_c)$:

$$\langle Q_{11\frac{l}{2}}\rangle \propto \frac{k_b^2}{k^2}[\langle j_2\rangle\Psi_2^2+3\sqrt{3}\langle j_4\rangle\Psi_2^4-\sqrt{182}\langle j_6\rangle\Psi_2^6], \quad (3)$$

$$\langle Q_{01\frac{l}{2}}\rangle \propto \langle Q_{11\frac{l}{2}}\rangle+\frac{k_b^2}{k^2}\sqrt{21}\langle j_4\rangle\Psi_4^4, \quad (4)$$

where Ψ_q^K is a structure factor of the chemical unit cell that is a linear sum of the atomic tensors $\langle T_{\pm q}^K\rangle$ that describe the asphericity of the Tb 4*f* electronic shell, where $\langle T_2^2\rangle$ equals the quadrupole moment, $\langle T_2^4\rangle$ the hexadecapole moment, and $\langle T_2^6\rangle$ the hexacontatetrapole moment. $\langle j_2\rangle$, $\langle j_4\rangle$, and $\langle j_6\rangle$ are Bessel function transforms of the radial distribution of the 4*f* electronic charge. In Eqs. (3) and (4), $(k_c/k)^2\sim 1$, and we neglect higher-order terms $(k_b/k)^4$ and $(k_b/k)^6$ as $k_b/k\ll 1$.

We discuss the configuration of the quadrupoles, but the order of the higher multipoles may alter also. When the 4*f* quadrupoles are aligned along [110] $(\phi_1=\phi_3=\frac{3}{4}\pi)$ as drawn in Fig. 3(b), $F_{01\frac{l}{2}}$ and $F_{11\frac{l}{2}}$ are both zero. When the 4*f* quadrupoles tilt toward the applied field with angle δ $(\phi_1=\frac{3}{4}\pi+\delta;\ \phi_3=\frac{3}{4}\pi-\delta)$, Fig. 3(c), $F_{01\frac{l}{2}}$ is finite and $F_{11\frac{l}{2}}$ remains zero. Neutron diffraction shows that in the AFM phase, the dipole moments tilt away from ⟨110⟩ with angle Δ, Fig. 3(d) $(\phi_1=\frac{3}{4}\pi-\Delta;\ \phi_3=\frac{3}{4}\pi-\Delta)$.[16] In this case, both $F_{01\frac{l}{2}}$ and $F_{11\frac{l}{2}}$ are zero in zero field, while under an applied field, Fig. 3(e), both become finite $(\phi_1=\frac{3}{4}\pi-\Delta+\delta;\ \phi_3=\frac{3}{4}\pi-\Delta-\delta)$.

Consequently, at 27 K, between $H=3.2$ and $H=3.5$ T, the magnetic and quadrupolar structure of TbB_2C_2 is characterized by phase IIa. The quadrupoles are aligned parallel to [110] as illustrated in Fig. 3(b) and are tilted in applied field as illustrated in Fig. 3(c). Above 3.5 T, the compound is characterized by phase IIb. The quadrupoles are tilted away from the [110] direction and neighboring atoms in the *ab* plane are tilted in opposite directions, as illustrated for $H=0$ in Fig. 3(d) and for $H\neq 0$ in Fig. 3(e). We show the phase diagram schematically in Fig. 3(a) and define a reorientation temperature T_R by the boundary between phases IIa and IIb. Resonant scattering at the Tb L_3 edge has shown a difference of ~0.7 K in ordering temperature between (102) and $(10\frac{3}{2})$ reflections.[17] The structure factor of the (102) reflection has a similar form as the $(11\frac{l}{2})$ reflection and confirms the occurrence of phase IIa succeeded by IIb upon cooling in zero field.

Multipole moment rotation in an applied field is linear for small δ and Δ [see Eq. (1)], hence the linear increase of the structure factor as observed at 15 K [see Fig. 2(b)]. The magnetic moment of the 4*f* shell tilts toward the direction of the magnetic field and the time-even multipole moments follow accordingly, giving the observed contrast. This shows that (i) the coupling between magnetic and quadrupole moments is rigid and (ii) the orbitals are already ordered in zero field, although with a ferroquadrupolar alignment. This is consistent with the result in Fig. 1(a) as the ferroquadrupolar alignment in zero field does not contribute to scattering at $(00\frac{l}{2})$, whereas in an applied field, due to the orbital rotation, time-even scattering dominates [Fig. 1(b)]. It is also in agreement with resonant x-ray diffraction at the Tb L_3 edge, which reports that quadrupoles are ordered below T_N in zero field.[17] We note that the weak intensity of $(01\frac{l}{2})$ in zero field as well as the resonant intensity observed around 1230 eV for π incident radiation in zero field [Fig. 1(a)] indicate a small deviation from ferroquadrupolar arrangement along *c*. This will be discussed later.

The normalized structure factor of $(01\frac{l}{2})$ and $(11\frac{l}{2})$ reflections at 5 T with $9\leqslant l\leqslant 17$ is presented in Fig. 4. They are equal within the experimental uncertainty which shows that Ψ_4^4 is small [Eqs. (3) and (4)]. The solid line corresponds to Eqs. (1) and (3) with $\Psi_2^4/\Psi_2^2=0.5$ and $\Psi_2^6/\Psi_2^2=0.5$ and shows that the intensity can be attributed to time-even x-ray diffraction. The dotted and dashed lines correspond to the

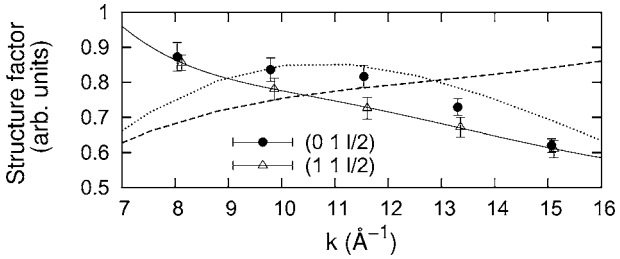

FIG. 4. Structure factor of $(01\frac{l}{2})$ and $(11\frac{l}{2})$ reflections at $B=5$ T and $T=2$ K. The solid line is a fit to Eq. (1), the dotted and dashed lines represent alternate B and Tb movement along *c*, respectively, as proposed for DyB_2C_2 by Refs. 9 and 10.

normalized structure factor of alternate B (Ref. 9) and Tb (Ref. 10) movements along the c axis, respectively. The limited range of k makes the determination of Ψ_q^x uncertain, and we cannot exclude an additional structural component due to B (or C) movement at 5 and 2 K. However, it is difficult to envisage how a structural transition can give two transition temperatures with smooth order parameter as recorded in Fig. 2(a). Thus, orbital order appears present independent of a significant structural transition in TbB_2C_2, verifying that the orbital interaction is mediated via the conduction electrons. A similar conclusion was reached for DyB_2C_2 from inelastic neutron scattering.[18]

With $\langle Q_{01\frac{l}{2}}\rangle = \langle Q_{11\frac{l}{2}}\rangle$ for a given field and temperature, the angle Δ is deduced from the ratio between $F_{01\frac{9}{2}}$ and $F_{11\frac{15}{2}}$. In addition, the quantity $\sin(2\delta)\langle Q_{hkl}\rangle$ follows from Eqs. (1) and (2), and δ has been estimated assuming $\langle Q_{hkl}\rangle$ is constant as a function of field and temperature. Both results are presented in Figs. 2(c) and 2(d). If $\langle Q_{hkl}\rangle$ increases with H, the actual values for δ are lower than presented in Fig. 2(d). Nevertheless, the increase in δ is gradual as a function of the applied field and reflects the orbital moment rotation.

The angle Δ is a result of the competition between the indirect Coulomb interaction and the magnetic exchange interaction between neighboring ions in the ab plane. The first interaction favors perpendicular alignment of the quadrupoles while the latter favors a parallel alignment. An increase in Δ is observed with H. This shows that the relative strength of the indirect Coulomb interaction *increases* as the quadrupoles rotate perpendicular to each other in an applied field. We note that the determination of Δ is robust against changes in $\langle Q_{hkl}\rangle$ with applied field.

If the observed nonresonant $(01\frac{9}{2})$ intensity in zero field is of orbital origin, it corresponds to $\delta = 1.0(3)°$. In zero field, δ is a measure of the AFQ interaction along c. In applied magnetic field along [110], we cannot distinguish between orbital rotation due to the magnetic moments and an increase in AFQ along c as both manifest themselves in an increase in δ.

We now discuss the resonant Bragg diffraction results. The $(00\frac{1}{2})$ diffracted intensity is relatively weak in zero applied field and appears magnetic in origin as witnessed by the relatively larger intensity for π-polarized x rays [Fig. 1(a)]. For scattering due to magnetic moments, $\sigma\sigma'$ is zero while $\pi\pi'$ is not. The energy profiles shown are expected to be insensitive to the magnetic structure, not to be confused with the total intensity that does depend on the magnetic structure. The drastic change with H indicates the presence of either an additional component of resonant scattering or a change in relative contribution of two different components of resonant scattering. The energy profile recorded in an applied magnetic field is similar to that recorded for the $(00\frac{1}{2})$ reflection in DyB_2C_2 in the AFQ phase.[19] There, the energy spectra with its interference like shape has been theoretically described due to an intra-atomic quadrupole interaction, which splits the core state. With such an ansatz, information on higher multipole moments were extracted. Here, we do not describe the data in such detail. However, the similarities in the spectra imply that for TbB_2C_2, under the influence of an applied magnetic field of 1 T, the $(00\frac{1}{2})$ reflection is dominated by a quadrupole contribution. This is consistent with the drastic change in the E2 resonance observed at the L_3 edge in applied field.[20]

The small nonzero delta in zero fields is consistent with the resonant intensity observed around 1230 eV for π incident radiation and zero applied field. This particular energy range of the spectrum appears to be a characteristic for orbital order. Interference between diffractions of magnetic and orbital origin prevents a simple interpolation between intensities, but nevertheless the magnitude of the intensity around 1230 eV appears in agreement with a 1° misalignment between neighboring Tb orbitals along c.

We now calculate the resonant scattering amplitudes for the orbital motif of TbB_2C_2 as drawn in Fig. 3(e). The following symmetry relations between the atomic spherical tensor of the Tb $4f$ shell $\langle T_q^K\rangle_d$ at site d are identified. The $4f$ shell at site 2(4) is a mirror image of the $4f$ shell at site 1(3) with reflection plane $(0.5a\ 0.5b\ 0)$. In addition, its moment is inverted. Note that applying a magnetic field in another direction will remove this symmetry constrain and results in different tensor contributions to the scattering. Correspondingly, a different azimuthal and energy dependence of the reflection is expected. Following the formalism of Lovesey *et al.*[15] we obtain for the structure factor of the $(00\frac{1}{2})$ $\Psi_q^K = \Sigma_d e^{ikd}\langle T_q^K\rangle_d$:

$$\Psi_q^K = [1-(-1)^K e^{-iq2\delta}]\langle T_q^K\rangle + (-1)^q e^{iq\pi/2}[1-(-1)^K e^{iq2\delta}]\langle T_q^K\rangle^*, \quad (5)$$

$$\Psi_{-q}^K = (-1)^q[1-(-1)^K e^{iq2\delta}]\langle T_q^K\rangle^* + e^{-iq\pi/2}[1-(-1)^K e^{-iq2\delta}]\langle T_q^K\rangle, \quad (6)$$

where $\langle T_q^K\rangle$ refers to atom 1. K equals 1 and 2 for magnetic and quadrupolar orders respectively. The $2/m$ site symmetry gives $K+q$ that is even, $-K \leqslant q \leqslant K$, and $\Psi_0^K = 0$.

The scattering amplitude for $E1$ process with the $(00\frac{1}{2})$ reflection in the scattering plane equals

$$F = \sum_{KQ} X_{-Q}^K \sum_q d_{Qq}^K(\pi/2) e^{iq\psi}\Psi_q^K, \quad (7)$$

where $-q \leqslant Q \leqslant q$, $d_{Qq}^K(\pi/2)$ is an element of rotation matrix or Wigner D function that rotates the sample to the reference frame of the experiment and ψ the azimutal angle. $\psi = 0°$ corresponds to the b axis in the scattering plane. The Bragg angle $\theta \simeq 45°$ and $\cos 2\theta \simeq 0°$,

$$F_{\sigma'\sigma} = \sin(2\psi)A_2^2, \quad (8)$$

$$F_{\pi'\sigma} = -i\cos\theta(\sin\psi - \cos\psi)A_1^1 - \sin\theta\cos 2\psi A_2^2, \quad (9)$$

$$F_{\sigma'\pi} = -F_{\pi'\sigma}, \quad (10)$$

$$F_{\pi'\pi} = i\sin 2\theta(\cos\psi + \sin\psi)A_1^1 - 0.5\sin 2\psi A_2^2, \quad (11)$$

where A_q^K is real and equals

$$A_1^1 = [\mathrm{Re}\langle T_1^1\rangle - \mathrm{Im}\langle T_1^1\rangle](1+\cos 2\delta) + [\mathrm{Re}\langle T_1^1\rangle + \mathrm{Im}\langle T_1^1\rangle]\sin 2\delta,$$

$$A_2^2 = 2\,\mathrm{Im}\langle T_2^2\rangle(1-\cos 4\delta) + 2\,\mathrm{Re}\langle T_2^2\rangle \sin 4\delta.$$

$\mathrm{Re}\langle T_q^K\rangle$ and $\mathrm{Im}\langle T_q^K\rangle$ are the real and imaginary parts of $\langle T_q^K\rangle$. $A_2^2=0$ for $\delta=0$, and orbital scattering is absent in zero field. For an azimuthal angle $\psi \simeq 45°$, Eqs. (8)–(11) simplify to

$$F_{\sigma'\sigma} = A_2^2,$$

$$F_{\pi'\sigma} = F_{\sigma'\pi} = 0,$$

$$F_{\pi'\pi} = i\sqrt{2}A_1^1 - 0.5A_2^2.$$

As A_1^1 is much smaller as A_2^2, the main difference between the σ and π incidence spectra is that the σ incidence intensity is expected to be approximately four times larger. This is in good agreement with the observation, considering that the azimuthal angle is not better defined than 5° in our experiment. Though the magnetic contribution is small, a closer look at the spectra shows that it is responsible for the slightly different shape of the π incidence spectra around 1238 eV, where a broadening of the central peak feature is observed when compared to the σ incident spectra. The resonant diffraction data therefore support the view of a strong induced orbital signal under applied fields consistent with the nonresonant diffraction data. It would be desirable to have more data under different magnetic fields and for different azimuthal angles, though this is beyond our experimental means.

In DyB_2C_2, the AFQ interaction is strongest along the *c* axis and a quasi-one-dimensional AFQ interaction has been reported.[21] From resonant scattering, it has been suggested that the buckling of the B and C sheets accompanying the orbital order and assisting the AFQ along *c* actually opposes the AFQ interaction in the plane, giving rise to the quasi-one-dimensional behavior.[19] Our findings suggest that the AFQ interaction in the plane dominates in TbB_2C_2 because the angle of Tb orbital misalignment in the plane equals 4° compared to 1° for out of plane (15 K, zero field).

In phase IIa, the orbitals are aligned as dictated by the magnetic order, i.e., all 4*f* orbitals are aligned parallel, also in the *ab* plane. This indicates that magnetocrystalline anisotropy is unlikely as the origin of the canting of the orbitals in phase IIb.

The increase in ordering temperature with applied field[11] is in line with an antiferroquadrupolar interaction which becomes stronger when the angle between the orbitals moves from parallel to perpendicular alignment. The magnetic moments interact via the polarized spins of the conduction electrons, while the multipolar moments interact via the charge density of the conduction electrons. In other words, charge screening by the conduction electrons changes when the 4*f* orbitals rotate, and, consequently, the magnitude of the quadrupole pair-interactions changes. This is consistent with the theoretical framework of Teitelbaum and Levy[3] where electric multipole coupling via the conduction electrons depends on the relative angular positions of the ion cores.

The occurrence of combined AFQ and AFM orderings below T_N is consistent with the quasidoublet ground state.[22] Removal of the degeneracy of a doublet ground state may account for one phase transition. Relaxation between the two singlets takes place above T_N, and the magnetic and quadrupolar moments fluctuate. The increased energy separation between the two singlets below T_N is due to the magnetic exchange interaction, but both the magnetic and quadrupolar moments of the ground state singlet are observed, and this is illustrated by this study.

V. CONCLUSION

In conclusion, no magnetic-field-induced ordering of quadrupoles exists in TbB_2C_2. The orbitals are already ordered in the AFM phase in zero field with a ferroquadrupolar motif. On increasing the applied field along [110], the Tb 4*f* magnetic moments rotate toward the field direction in a gradual manner. The quadrupole moment is rigidly coupled to the magnetic moment and follows this rotation. Neighboring Tb 4*f* orbitals move from parallel to perpendicular alignment and the quadrupolar pair-interaction increases, witnessed by an increase of angle Δ between neighboring quadrupoles. This study shows that the quadrupolar pair-interaction depends on the specific orientation of the orbitals as predicted for indirect Coulomb interaction via the conduction electrons and can be manipulated with an applied field.

ACKNOWLEDGMENTS

We thank S. W. Lovesey for valuable discussion. This work was supported by the Swiss National Science Foundation and by a Grant-in-Aid for Scientific Research from the Japan Society for the Promotion of Science. This work was in part performed at the SLS of the Paul Scherrer Institut, Villigen PSI, Switzerland.

[1] S. Grenier, J. P. Hill, D. Gibbs, K. J. Thomas, M. v. Zimmermann, C. S. Nelson, V. Kiryukhin, Y. Tokura, Y. Tomioka, D. Casa, T. Gog, and C. Venkataraman, Phys. Rev. B **69**, 134419 (2004).
[2] T. Takimoto, Phys. Rev. B **62**, R14641 (2000).
[3] H. H. Teitelbaum and P. M. Levy, Phys. Rev. B **14**, 3058 (1976).
[4] P. M. Levy, P. Morin, and D. Schmitt, Phys. Rev. Lett. **42**, 1417 (1979).
[5] T. Onimaru, T. Sakakibara, N. Aso, H. Yoshizawa, H. S. Suzuki, and T. Takeuchi, Phys. Rev. Lett. **94**, 197201 (2005).
[6] A. Kiss and P. Fazekas, Phys. Rev. B **71**, 054415 (2005).
[7] H. Adachi, H. Kawata, M. Mizumaki, T. Akao, M. Sato, N. Ikeda, Y. Tanaka, and H. Miwa, Phys. Rev. Lett. **89**, 206401 (2002).
[8] T. Tanaka, U. Staub, K. Katsumata, S. W. Lovesey, L. E. Lorenzo, Y. Narumi, V. Scagnoli, S. Shimomura, Y. Tabata, Y. Onuki, Y. Kuramoto, A. Kikkawa, T. Ishikawa, and H. Kitamura, Physica B **378-380**, 367 (2006).
[9] Y. Tanaka, T. Inami, T. Nakamura, H. Yamauchi, H. Onodera, K. Ohoyama, and Y. Yamaguchi, J. Phys.: Condens. Matter **11**,

L505 (1999).
[10] K. Hirota, N. Oumi, T. Matsumura, H. Nakao, Y. Wakabayashi, Y. Murakami, and Y. Endoh, Phys. Rev. Lett. **84**, 2706 (2000).
[11] K. Kaneko, H. Onodera, H. Yamauchi, T. Sakon, M. Motokawa, and Y. Yamaguchi, Phys. Rev. B **68**, 012401 (2003).
[12] K. Kaneko, S. Katano, M. Matsuda, K. Ohoyama, H. Onodera, and Y. Yamaguchi, Appl. Phys. A **74**, S1749 (2002).
[13] U. Staub, V. Scagnoli, A. M. Mulders, K. Katsumata, Z. Honda, H. Grimmer, M. Horisberger, and J. M. Tonnerre, Phys. Rev. B **71**, 214421 (2005).
[14] V. Scagnoli, U. Staub, A. M. Mulders, M. Janousch, G. I. Meijer, G. Hammerl, J. M. Tonnerre, and N. Stojic, Physica B **378-380**, 367 (2006).
[15] S. W. Lovesey, E. Balcar, K. S. Knight, and J. Fernández-Rodríguez, Phys. Rep. **411**, 233 (2005).
[16] K. Kaneko, H. Onodera, H. Yamauchi, K. Ohoyama, A. Tobo, and Y. Yamaguchi, J. Phys. Soc. Jpn. **70**, 3112 (2001).
[17] D. Okuyama, T. Matsumura, H. Nakao, Y. Murakami, H. Onodera, A. Tobo, Y. Wakabayashi, and H. Sawa, J. Phys. Soc. Jpn. **74**, 1566 (2005).
[18] U. Staub, A. M. Mulders, O. Zaharko, S. Janssen, T. Nakamura, and S. W. Lovesey, Phys. Rev. Lett. **94**, 036408 (2005).
[19] A. M. Mulders, U. Staub, V. Scagnoli, S. W. Lovesey, E. Balcar, T. Nakamura, A. Kikkawa, G. van der Laan, and J. M. Tonnerre, J. Phys.: Condens. Matter **18**, 11195 (2006).
[20] D. Okuyama, T. Matsumura, H. Nakao, Y. Murakami, Y. Wakabayashi, A. Tobo, and H. Onodera, Physica B **378-380**, 488 (2006).
[21] K. Indoh, A. Tobo, K. Ohoyama, and H. Onodera, J. Phys. Soc. Jpn. **73**, 1554 (2006).
[22] M. Maino, A. Tobo, and H. Onodera, J. Phys. Soc. Jpn. **74**, 1838 (2005).